Thermal Stability of Europium(III) Chelate Encapsulated by Sol-Gel Glass

E. Kin, T. Fukuda, S. Yamauchi, Z. Honda, H. Ohara*, T. Yokoo*, N. Kijima* and N. Kamata

Saitama University, 255 Shimo-Okubo, Sakura-ku, Saitama-shi, Saitama 338-8570, Japan

* Mitsubishi Chemical Group, Sci. and Tech. Res. Center, Inc., 1000 Kamoshida-cho, Aoba-ku, Yokohama 227-8502, Japan

Corresponding author: F. Fukuda

e-mail: fukuda@fms.saitama-u.ac.jp

Tel/Fax:+81-48-858-3526

Abstract

In order to improve the stability of high color-purity red phosphors for ultraviolet excitation, we encapsulated an Eu-chelate, $Eu(HFA)_3(TPPO)_2$, by sol-gel derived glass networks and studied its thermal stability as well as photoluminescence (PL) characteristics. The PL quantum yield of an encapsulated sample was ten times higher than that without encapsulation after annealing at 160 °C for 2 hours in air. Three-dimensional glass networks with a sufficient density were shown to reduce thermal quenching of $Eu(HFA)_3(TPPO)_2$. Therefore, it is revealed that the surface coating of luminous chelates by sol-gel glasses is an effective way of inorganic and organic hybridization for high-stability of chelate bonding against free-oxygen and water.

Keyword: Composite materials, Sol-gel processes, Optical properties, Luminescence,

1. Introduction

Though the typical f-f transition of trivalent Eu ions matches the wavelength of high color-purity red, concentration quenching of Eu ions limits the available total emission intensity. A combination with an appropriate ligand to form Eu-chelate, or Eu-complex, improves absorption strength per each Eu ion and solves the problem of concentration quenching due to the increase of inter-molecular distances. Such Eu-chelates as $Eu(TTA)_3Phen$ [TTA: thenoyltrifluoronacetone, Phen: 1,10-phenanthroline] and $Eu(HFA)_3(TPPO)_2$ [HFA: hexafluoroacetylacetonato, TPPO: 1,2-phenylenebis(diphenylphosphine oxide）] etc., therefore, have attracting attention recently for white LED applications.

In comparison with conventional inorganic phosphor materials, on the other hand, the robustness of organic molecules is lower due to the bond strength of molecules fundamentally [4-6]. This fact requires us an urgent way of improving reliability of luminous chelates at actual condition. Encapsulation [7, 8] of organic molecules against ambient oxygen and water by inorganic materials are one of crucial technological issues on inorganic-organic hybridization [9, 10] for improving reliability and widening applications of light emissive materials [11, 12].

In this paper, we demonstrate higher thermal stability of Eu(III) chelates, $Eu(HFA)_3(TPPO)_2$, encapsulated by sol-gel derived silica glass. Since the sol-gel synthesis including a final annealing process could be performed at temperatures below 150 °C, it is free from the thermal decomposition of $Eu(HFA)_3(TPPO)_2$ during the fabrication process. In addition to maintain the initial photoluminescence (PL) quantum yield, the glass network is expected to protect the Eu-chelate against free oxygen and water, thus improve thermal and long term durability of PL intensity under atmospheric condition.

We studied the influence of the thermal treatment on optical properties of sol-gel glass encapsulated $Eu(HFA)_3(TPPO)_2$ by comparing absorption, PL, PL excitation (PLE) spectra and PL quantum yield measurements. An improvement in the reliability due to the glass encapsulation was shown by ten times higher PL quantum yield after annealing at 160 °C for 2 hours in air, and by monitoring the long-term decrease in PL intensity under constant UV light irradiation. Combining superior efficiency and functionality of organic molecules with transparent and protective glass matrix opens a wider field of effective inorganic-organic hybridized materials and devices.

2. Experimental

Figure 1 shows the flowchart of encapsulating $Eu(HFA)_3(TPPO)_2$ by so-gel glasses. At first, 1.5 mmol $Eu(HFA)_3(TPPO)_2$ powder was added to the encapsulating agent of 1.0 mol n-propyltrimethoxy- silane (PTMS) and 0.5mol dimethyldimethoxysilane (DEDMS). The solution was mixed at 25 °C for 24 hours until $Eu(HFA)_3(TPPO)_2$ was completely dissolved. Then, the solution was injected into 25 mol distilled water, 5 mol ethanol, and 0.053 mol acetic acid. The solution was subsequently mixed at 80 °C for 2 hours and 100 °C for 3 hours to remove distilled water, organic solvent and ethanol. The rotation speed was maintained 400 rpm with a magnetic stirrer for all the mixing processes. Finally, the solution was

dipped on a glass substrate and spin-coated at the rotation speed of 2,000 rpm for 60 seconds. Typical thickness of the spin-coated film was 2000 nm.

To investigate the thermal stability of the sol-gel glass encapsulated $Eu(HFA)_3(TPPO)_2$, samples were annealed at the temperature ranging from 120 to 220 °C using a hotplate for 2 hours (sample A) in air. For comparison, $Eu(HFA)_3(TPPO)_2$ powder was dissolved in tetrahydrofuran (THF), and the solution was also spin-coated on glass substrates. At each annealing condition of the sample A, we prepared two spin-coated films without encapsulation; one is annealed in air (sample B) and the other is annealed in dry nitrogen (sample C), respectively. The organic solvent of THF is easily removed by the annealing process over 120 °C owing to its low boiling point.

The PL quantum yield was measured by luminance quantum yield measurement system (QEMS-2000, Systems Engineering Inc.), which consists of a calibrated integrated sphere and exciting violet laser diode at the wavelength of 385 nm. The PL quantum yield was obtained by a comparison between the PL spectrum of the sample and the emission spectrum of the excited laser diode. UV-Vis and IR absorption spectra were recorded with a UV/VIS spectrophotometer (V-550, JASCO) and a FT-IR spectrometer (XXXX, JASCO). PL and PLE spectra were measured by the luminance spectrometer (FluoroMax, Horiba Jovin Yvon).

3. Results and Discussion

3.1 PL Intensity Quenching

Prior to the glass encapsulation, PL and PLE spectra of $Eu(HFA)_3(TPPO)_2$ were measured by spin-coated samples B and C. The luminous transition of $Eu(HFA)_3(TPPO)_2$ originates from $^5D_0 \rightarrow {}^7F_J$ (J=1, 2, 3, 4) in Eu^{3+} [3, 13]. The chelate showed a distinct peak of $^5D_0$-$^7F_2$ transition of 613 nm in the PL spectrum shown in Fig. 2 (sample B) and Fig. 3 (sample C), respectively, resulting in the high color-purity as a red component. With increasing an annealing temperature, the PL intensity quenching of sample B (treated in air) became pronounced over that of sample C (treated in dry nitrogen) as shown in those figures. In the FT-IR spectrum of $Eu(HFA)_3(TPPO)_2$ thermally treated 2 hours in air, the absorption due to C-F bond oscillation around 1220-1255 cm^{-1} decreased with increasing the annealing temperature as shown in Fig. 4.

These results proved that the presence of oxygen and/or water in the atmosphere modified and/or decomposed the molecular conformation of ligands, and accelerated the PL intensity quenching during the high temperature treatment. An encapsulation of the chelate against environmental oxygen and water is considered to be advantageous for reducing the PL intensity quenching and improving the thermal stability.

A mixture of PTMS and DEDMS was chosen rather than PTMS alone, because DEDMS makes hydrolysis easier than PTMS. The function of DEDMS is to form a more flexible linear network than the one obtained by hydrolysis of PTMS alone. The Eu chelate is incorporated in the matrix at the same time

as the hydrolysis and condensation reactions of silane starts, not after the sol-gel glass formation has finished. Therefore, we could obtain transparent and nearly crack-free film by the combination of PTMS and DEDMS used as the formation of three-dimensional dense network around $Eu(HFA)_3(TPPO)_2$.

3.2 Absorption Spectra

Similar to the PL and PLE spectra, UV-Vis absorption spectra of all samples at each annealing temperature were measured and their peak values were determined. In Fig. 5, we show the annealing temperature dependence of the normalized peak absorbance of samples A, B and C, respectively. The peak absorbance of sample A is normalized by its value at 140 ℃, since the effective thickness is an order of magnitude different from those of samples B and C, while the ordinate for samples B and C is normalized by the common value of the sample C at 140 ℃.

The 350 nm absorption band, shown in Fig. 2 for example, is attributed to the absorption of ligand of $Eu(HFA)_3(TPPO)_2$, and its decrease with increasing annealing temperature implies the thermal decomposition of the ligand bonding. In sample A, the change in the normalized absorbance was not so dominant below 200 ℃: The value at 200 ℃ still kept 80%. The normalized absorbance of sample C, on the other hand, decreased down to 50% at 180 ℃. For sample B, the peak absorbance at 140 ℃ itself was only 40% of that in sample C.

This result indicates that the decomposition of the chelate bonding during thermal annealing in air is reduced by encapsulating sol-gel glass networks in sample A.

In Fig. 6, the PL quantum yields of all samples were plotted as a function of annealing temperature between 120 and 220 ℃. With increasing annealing temperature, the quantum yield of sample B (annealed in air) decreased rapidly, e. g. 12% at 140 ℃, while that of sample C (annealed in dry nitrogen) and the encapsulated sample A (annealed in air) showed improved values. In sample A, the PL quantum yield remained equal to the original value of c. 50 % up to 140 ℃, and then decreased monotonously. The sample C showed similar but somewhat lower values when compared with that of sample A. Values of samples A and C at 160 ℃ were 35 and 32%, respectively. It is noted that the sol-gel glass coating plays an important role in reducing the PL intensity quenching of the Eu chelate when annealed in air at the temperature region below 200 ℃.

The absorbance represents an efficiency of light absorption process, while the PL quantum yield implies the efficiency of spontaneous light emission after absorbing a same amount of photons. Comparing the result with that of peak absorbance in Fig. 5, it is clear that a nonradiative loss mechanism after absorption process takes place even in the sample A at the annealing temperature above 160 ℃. We consider it to be a nonradiative recombination via a surface defect, possibly dangling bonds or residual –OH oscillations, of sol-gel glass. Such surface defects might be reduced by further optimization of sol-gel reaction conditions. Presently only note that the ordinate in Fig. 6 is an absolute value: The highest values of encapsulated sample A among others even before detailed optimization implies a

possibility of the method with further improvement.

3.2 Stabilization of $Eu(HFA)_3(TPPO)_2$ by Sol-Gel Glass

In Fig. 7, we show a long term PL intensity variation of Eu-chelates with and without glass encapsulation. Here, samples were irradiated by a constant UV excitation light of 350 nm with the intensity of 6.95 mW/cm^2 and their peak PL intensities of 613 nm corresponding to the $^5D_0$-$^7F_2$ transition of Eu^{3+} were monitored. The spin-coated $Eu(HFA)_3(TPPO)_2$ film annealed at 120 ℃ in air showed monotonic decrease in PL intensity, down to 57% at 60 min. The glass-encapsulated $Eu(HFA)_3(TPPO)_2$, annealed at 120 ℃ in air, on the other hand, showed superior value of 70% after the same period. These results exemplified also the effect of encapsulation on the long term stability of the Eu-chelate by protecting against free oxygen and water.

4. Conclusions

We encapsulated a high color-purity luminescent chelate, $Eu(HFA)_3(TPPO)_2$, by a sol-gel glass and studied its thermal stability based on absorption, PL, PLE and the PL quantum yield measurements. A distinct reduction of thermal quenching in the PL quantum yield after annealing at 160 °C, and an improved long term stability of PL intensity under constant UV excitation were successfully achieved by coating the sol-gel glass. These results were attributed to the protection effect of a three dimensional glass networks against free oxygen and/or water for the sake of preserving chelate bonding at the annealing temperature region below 200 °C. The encapsulation method opens a field of effective inorganic-organic hybridized materials and devices, combining superior functionality of organic molecules with transparent and protective nature of glass matrix.

Acknowledgements

The authors would like to thank Prof. Y. Taniguchi, Associate Prof. M. Ichikawa, and Mr. S. Kanazawa (Shinshu University) for the measurement of PL quantum yield.

References

[1] H. Li, S. Inoue, K.I. Machida, G.Y. Adachi, Chem. Mater. 11 (1999) 3171 -3176.

[2] Q. Ling, M. Yang, Z. Wu, X. Zhang, L. Wang, W. Zhang, Polymer 42 (2001) 4605-4610.

[3] J. Fang, D. Ma, Appl. Phys. Lett. 83 (2003) 4041-4044.

[4] E. Vaganova, R. Reisfeld, S. Yitzchaik, Opt. Mater. 24 (2003) 69-76.

[5] L.C. Codes da Silva, T.S. Martins, M.Santos Filho, E.E.S. Teotônio, P.C. Isolani, H.F. Brito, M.H. Tabacniks, M.C.A. Fantini, J.R. Matos, Micro. Meso. Mater. 92 (2006) 94-100.

[6] M. Xiao, P.R. Selvin, J. Am. Chem. Soc. 123 (2001) 7067-7073.

[7] Y. Wang, F. Caruso, Chem. Mater. 17 (2005) 953-961.

[8] M. Aslam, L. Fu, S. Li, J. Colloid. Interface Sci. 290 (2005) 444-449.

[9] Y. Terui, S. Ando, High Performance Polymers 18 (2006) 825-836.

[10] F Li, J Li, S.S. Zhang, Talanta 74 (2008) 1247-1255.

[11] C.J. Liang, D. Zhao, Z.R. Hong, D.X. Zhao, X.Y. Liu, W.L. Li, J.B. Peng, J.Q. Yu, C.S. Lee, S.T. Lee, Appl. Phys. Lett. 76 (2000) 67-69.

[12] R. Gupta, N.K. Chaudhury, Biosens. Bioelectron. 22 (2007) 2387-2399.

[13] H. Eilers, B.M. Tissue, Chem. Phys. Lett. 251 (1996) 74-78.

[14] T. Mohanty, N.C. Mishra, S.V. Bhat, P.K. Basu, D.Kanjilal, J. Phys. D: Appl. Phys. 36 (2003) 3151-3155.

[15] L. Skuja, M. Hirano, H. Hosono, K. Kajihara, Phys. Sta. Sol. C 2 (2005) 15-24.

Figure Captions

Fig. 1 Flowchart of encapsulating $Eu(HFA)_3(TPPO)_2$ by sol-gel glasses.

Fig. 2 PL and PLE spectra of $Eu(HFA)_3(TPPO)_2$ spin-coated film (thermal treatment of X hours in air). Wavelength of monitoring in PLE and that of excitation in PL were 613 and 400 nm, respectively.

Fig. 3 PL and PLE spectra of $Eu(HFA)_3(TPPO)_2$ spin-coated film (thermal treatment of X hours in N_2). Wavelength of monitoring in PLE and that of excitation in PL were 613 and 400 nm, respectively.

Fig. 4 The FT-IR(Fourier transform infrared) absorption spectrum of $Eu(HFA)_3(TPPO)_2$ thermally treated 2 hours in air.

Fig. 5 Normalized absorbance of an encapsulated $Eu(HFA)_3(TPPO)_2$ (solid curve, sample A) and spin-coated $Eu(HFA)_3(TPPO)_2$ heated in N_2 and in air (dashed curve, sample C and dotted curve, sample B), respectively.

Fig. 6 PL quantum yield vs. annealing temperature for the encapsulated sample A (solid curve), and the spin-coated samples B (dotted curve) and C (dashed curve) with annealing in air and in nitrogen, respectively.

Fig. 7 PL intensity change of glass-encapsulated and without encapsulation samples under 350 nm excitation. The optical intensity of excited light was 6.95 mW/cm^2.

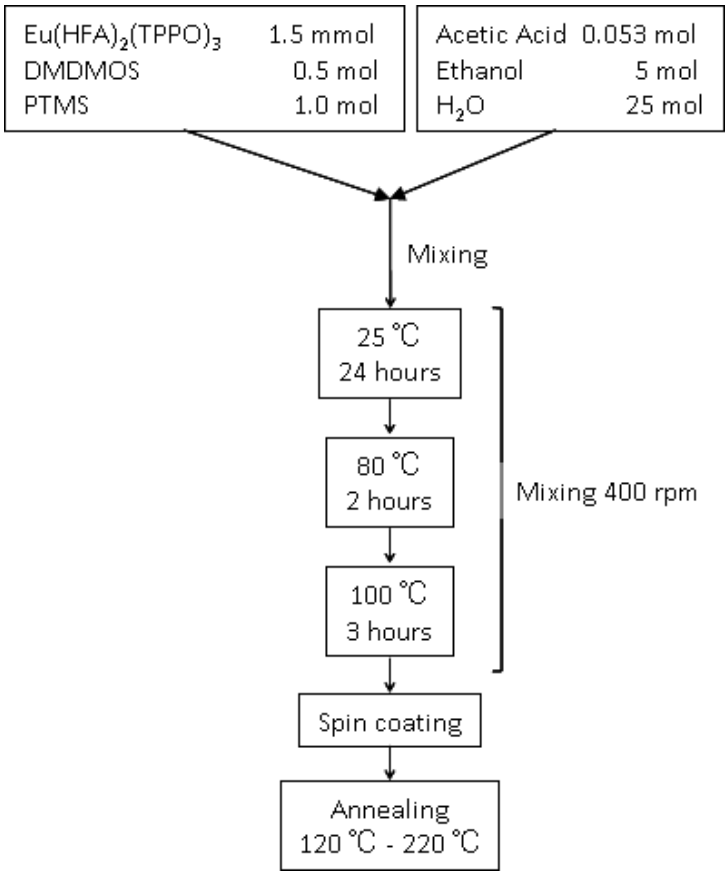

Fig. 1 Flowchart of encapsulating $Eu(HFA)_3(TPPO)_2$ by sol-gel glasses.

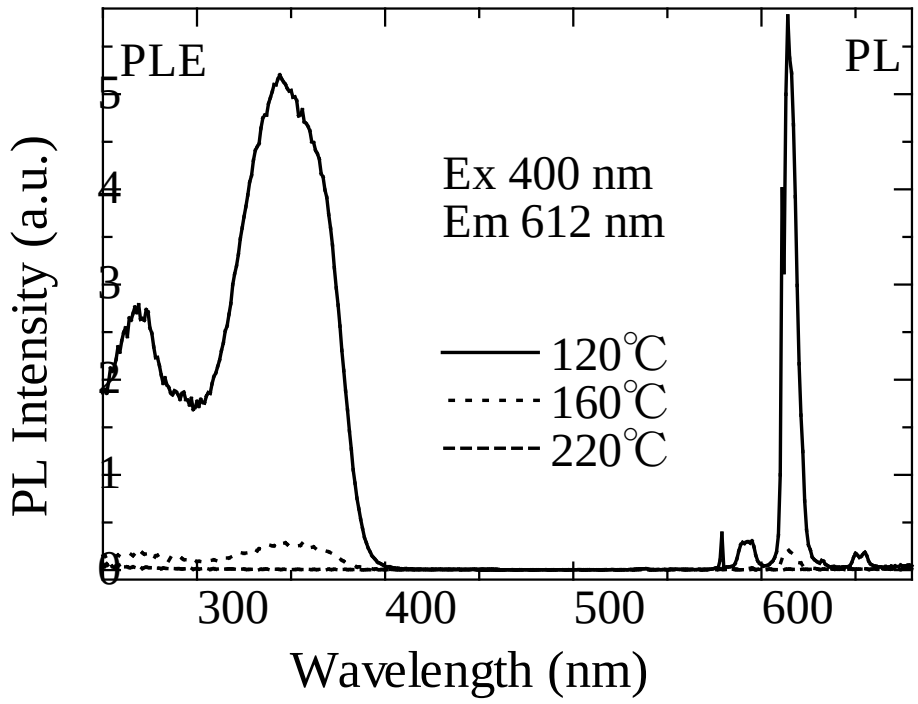

Fig. 2 PL and PLE spectra of $Eu(HFA)_3(TPPO)_2$ spin-coated film (thermal treatment of 2 hours in air). Wavelength of monitoring in PLE and that of excitation in PL were 613 and 400 nm, respectively.

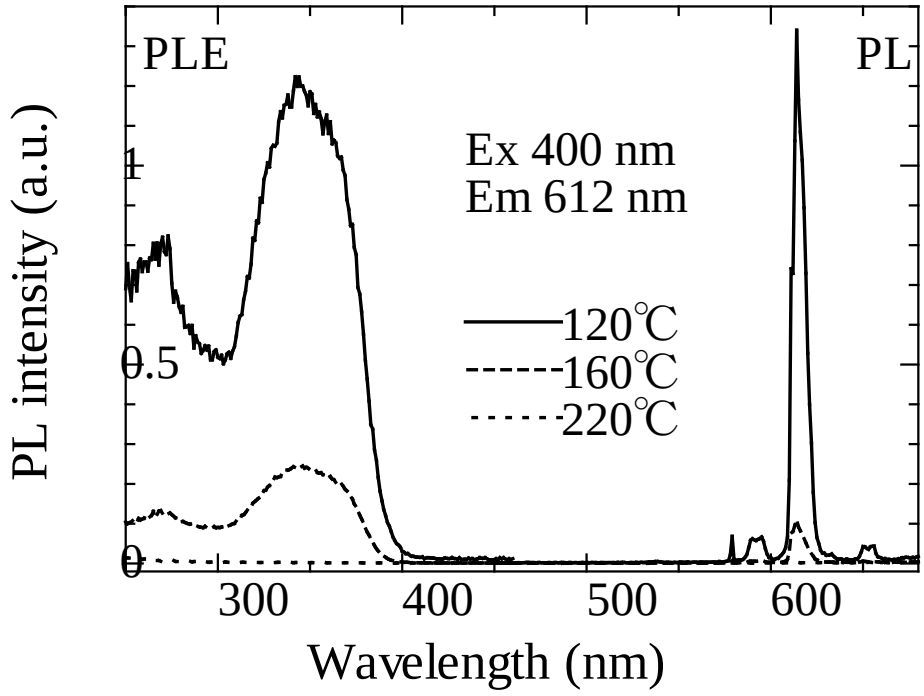

Fig. 3 PL and PLE spectra of $Eu(HFA)_3(TPPO)_2$ spin-coated film (thermal treatment of 2 hours in N_2). Wavelength of monitoring in PLE and that of excitation in PL were 613 and 400 nm, respectively.

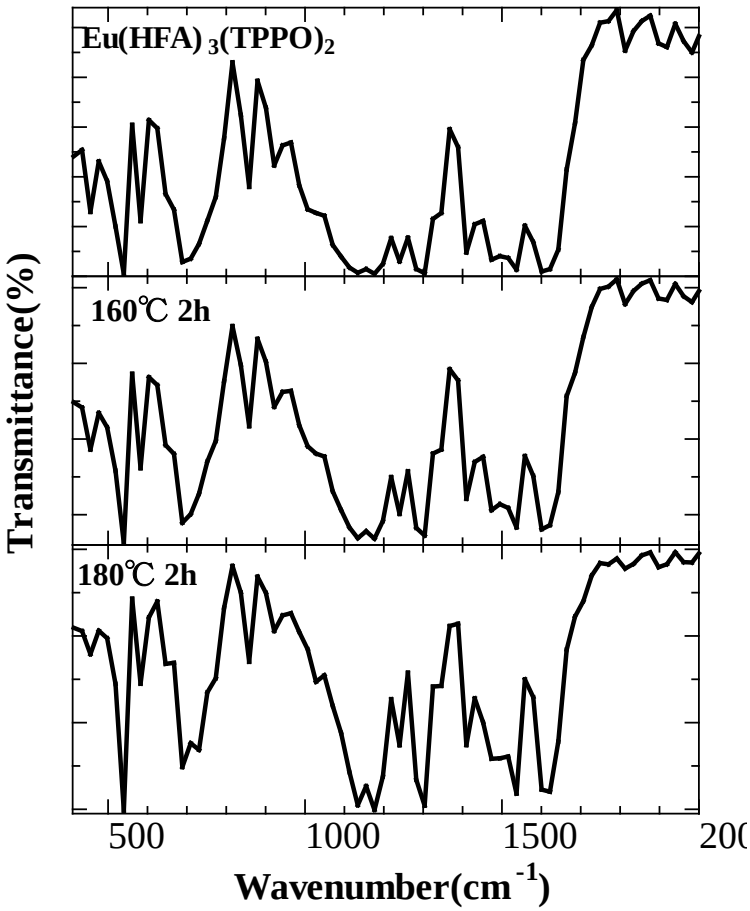

Fig. 4 The FT-IR absorption spectra of $Eu(HFA)_3(TPPO)_2$ thermally treated 2 hours in air.

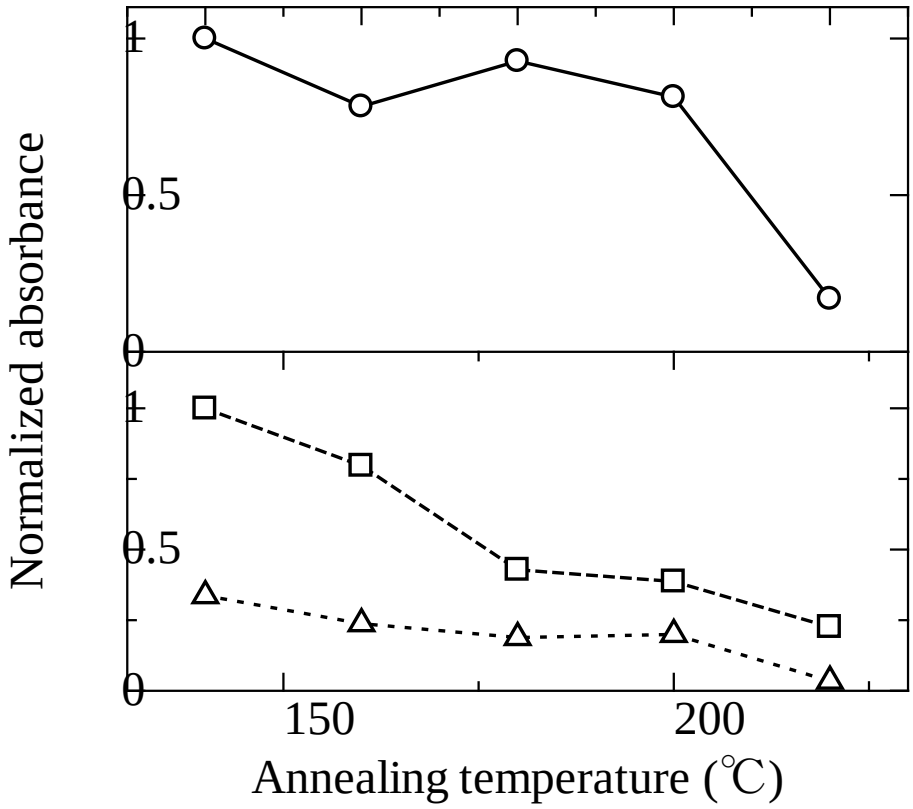

Fig. 5 Normalized absorbance of an encapsulated $Eu(HFA)_3(TPPO)_2$ (solid curve, sample A) and spin-coated $Eu(HFA)_3(TPPO)_2$ heated in N_2 and in air (dashed curve, sample C and dotted curve, sample B), respectively.

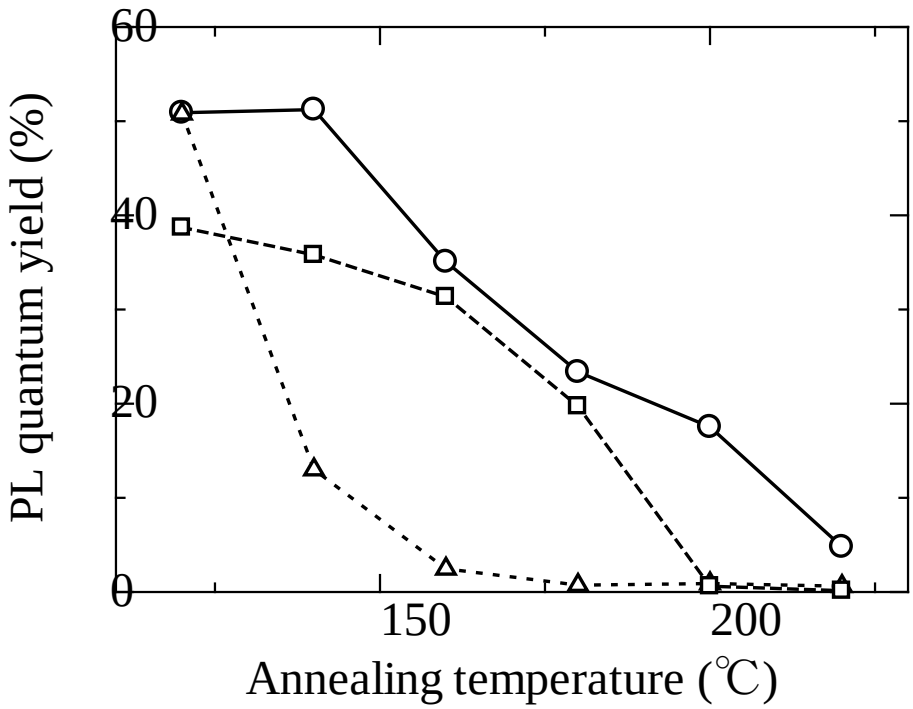

Fig. 6 PL quantum yield vs. annealing temperature for the encapsulated sample A (solid curve), and the spin-coated samples B (dotted curve) and C (dashed curve) with annealing in air and in nitrogen, respectively.

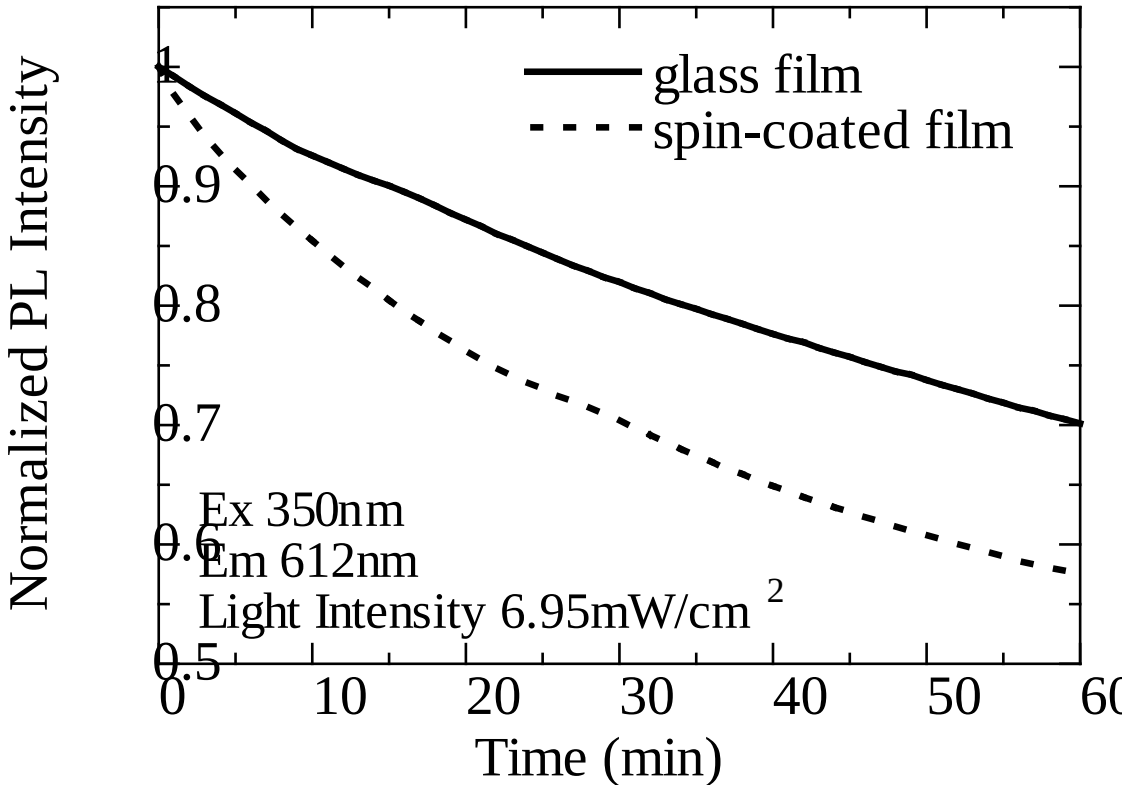

Fig. 7 PL intensity change of glass-encapsulated and without encapsulation samples under 350 nm excitation. The optical intensity of excited light was 6.95 mW/cm^2.